Optimal weighted networks of phase oscillators for synchronization

Takuma Tanaka*
Department of Morphological Brain Science, Graduate School of Medicine, Kyoto University, Kyoto, Japan

Toshio Aoyagi
Department of Applied Analysis and Complex Dynamical Systems, Graduate School of Informatics, Kyoto University, Kyoto, Japan and CREST, JST, Saitama, Japan

(Received 30 March 2008; revised manuscript received 12 August 2008; published 20 October 2008)

The phase order parameter of oscillators on a network is optimized using two different sets of constraints. First, the maximization is achieved by adjusting the coupling strengths among the oscillators without changing the total coupling strength and the natural frequencies of the oscillators. This optimization reveals that a stronger weight tends to be assigned to a connection between two oscillators with greatly different natural frequencies. Second, we vary both coupling strengths and natural frequencies while maximizing the phase order and minimizing the penalty function which prevents the natural frequencies of the oscillators from taking the same value. This optimization reveals that a large total coupling strength makes oscillators take two natural frequencies (two-group state), whereas a small total coupling strength facilitates the convergence of natural frequencies to one single value (one-group state). Small and large penalty parameters make the optimized network take the one- and two-group states, respectively. This phase transition is observed in all-to-all, lattice, and scale-free networks although the clustering coefficient of the strongest links in the optimized network reflects the difference of the underlying network topologies.

DOI: 10.1103/PhysRevE.78.046210 PACS number(s): 05.45.Xt, 64.60.aq, 87.55.de

I. INTRODUCTION

Collective phenomena of oscillatory elements underlie a large number of fundamental problems in physical, biological, chemical, and social systems. The method of phase description is effective in analyzing these systems, and the resultant systems of coupled phase oscillators yield powerful theoretical tools applicable to understanding synchronization observed in various real-world systems [1]. In its simplest solvable form, the evolution of the phase $\phi_i(t)$ of oscillator i $(i=1,\ldots,N)$ is governed by the equation

$$\frac{d\phi_i}{dt} = \omega_i + \frac{K}{N}\sum_{j=1}^{N} \sin(\phi_j - \phi_i), \tag{1}$$

where ω_i is the natural frequency of oscillator i and K is the coupling strength. Because each oscillator in Eq. (1) is uniformly coupled to all oscillators in the system, this system is called a globally coupled phase oscillator system with mean-field interaction. The degree of synchronization is measured by the order parameter defined as

$$R = \frac{1}{N}\sqrt{\left(\sum_i \cos\phi_i\right)^2 + \left(\sum_i \sin\phi_i\right)^2}.$$

Kuramoto showed that the globally coupled phase oscillator system exhibits a transition from an incoherent state to a synchronized state at a critical coupling strength K_c. In other words, the order parameter R takes nonzero values above K_c, whereas R vanishes below K_c. This type of transition was later reported for globally coupled phase oscillator systems with more general coupling functions. Systems with coupling functions containing only odd harmonics exhibit transitions from an incoherent state to a synchronized state at a critical coupling strength [2].

Since the classical work by Kuramoto, the system of phase oscillators has been a widely studied topic in nonlinear physics [3], and recently, several groups have moved attention to the investigation of oscillator systems on more complex network structures, such as small world networks and scale-free networks [4–9]. Moreno *et al.* [4] numerically simulated the behavior of oscillators on scale-free networks whose dynamics are governed by the evolution of the equation

$$\frac{d\phi_i}{dt} = \omega_i + K\sum_{j\in I(i)} \sin(\phi_j - \phi_i),$$

where $I(i)$ is the set of neighbors of oscillator i. They reported that the transition to the synchronized state occurred at a smaller value of the coupling strength K than in a system of globally coupled oscillators. Theoretical work by Ichinomiya [6] showed that the critical coupling constant at which transition occurs becomes 0 in random scale-free networks with degree distribution $P(k)\propto k^{-\gamma}$, if $2<\gamma\leqslant 3$. A more recent report compared the synchronizability of scale-free networks and Erdös-Renyi networks [9], and concluded that oscillators on scale-free networks are more readily synchronized than on Erdös-Renyi networks for small values of K, whereas for large values of K, the reverse is true.

In these previous studies, the networks had a uniform coupling strength K. However, in real-world networks, the coupling strengths (called connection weights W_{ij} in the terminology of networks), are generally not uniform but potentially take any positive value depending on the link

*ttakuma@mbs.med.kyoto-u.ac.jp

[10–12]. Investigations of synchronization on these general weighted networks have been limited to oscillator systems in the form

$$\dot{\mathbf{x}}_i = \mathbf{F}(\mathbf{x}_i) - \sigma \sum_{j=1}^{N} G_{ij}\mathbf{H}[\mathbf{x}_j],$$

where $\dot{\mathbf{x}}=\mathbf{F}(\mathbf{x})$ governs the dynamics of oscillator i, $\mathbf{H}[\mathbf{x}]$ is a linear function, σ is the coupling strength, and G is the coupling matrix [13,14]. Phase oscillator systems, which cannot be written in this form because the oscillators are coupled by a nonlinear function, have not been studied on these general weighted networks.

In this paper, we will investigate the optimal weighted network of phase oscillators for synchronization by focusing on the order parameter R. This endeavor requires many complicated questions to be answered, among them the questions of how large the coupling strength assigned to each link should be for better synchronization. We attempt to answer this question by estimating how each coupling strength and natural frequency contribute to the facilitation of synchronization of an oscillator for a given network structure. Changing the weight of links in a way that the order parameter increases, we can obtain the weighted network optimized for synchronization. Examining the weight obtained through optimization will allow us to understand the essential conditions that must be met for the synchronization of oscillators on weighted networks. In this paper, we first derive the optimization algorithm to maximize the order parameter R by using the steepest gradient method and then present numerical results showing the successful optimization of network weights in the case of all-to-all, lattice-type, and scale-free connection.

II. ALGORITHM

A. Optimization with respect to coupling strength

We derive here the algorithm to obtain the coupling strengths so that the optimization function

$$Q_1 = R^2 \tag{2}$$

is maximized for coupled Kuramoto oscillators. We use the optimization function Q_1 instead of R to simplify the calculation. The dynamics of the oscillators are described by

$$\frac{d\phi_i}{dt} = \omega_i + \sum_j a_{ij}K_{ij}\sin(\phi_j - \phi_i) \quad (i = 1, \ldots, N), \tag{3}$$

where ω_i is the natural frequency of oscillator i, a_{ij} is the adjacency matrix (1 if oscillators i and j are connected and 0 otherwise), and K_{ij} is the coupling strength between oscillators i and j. We maximize Q_1 under the constraint

$$\sum_{ij} K_{ij}^{\alpha} = K_{\text{total}}^{\alpha}, \tag{4}$$

where α and K_{total} are constant parameters. Each summation for K_{ij} is assumed to be taken over all (i,j), where $1 \leqslant i \leqslant N$ and $1 \leqslant j \leqslant N$. Thus, the L^{α} norm of the coupling strength is fixed to K_{total}. The constraint Eq. (4) is essential because without this constraint the coupling strength K_{ij} can grow without limit. We assume that the connection is symmetric, that is, $a_{ij}=a_{ji}$ and $K_{ij}=K_{ji}$. In the following, we assume that N oscillators in the system are phase locked, and hence the frequency of an oscillator is equal to the average of the frequencies of the oscillators,

$$\frac{1}{N}\sum_i \frac{d\phi_i}{dt} = \frac{1}{N}\sum_i \omega_i + \frac{1}{N}\sum_{ij} a_{ij}K_{ij}\sin(\phi_j - \phi_i) = \frac{1}{N}\sum_i \omega_i = \Omega,$$

where Ω is the average of the natural frequencies. Therefore, the equation

$$\omega_i + \sum_j a_{ij}K_{ij}\sin(\phi_j - \phi_i) = \Omega$$

holds for the system considered in this paper.

First, we derive the steepest gradient of Q_1 with respect to K_{ij}. When the coupling strength K_{ij} is changed to $K_{ij}+\Delta K_{ij}$, the difference of a phases $\phi_j-\phi_i$ between oscillators i and j changes to $\phi_j+\Delta\phi_j-\phi_i-\Delta\phi_i$, which is a solution of

$$\omega_i + \sum_j a_{ij}(K_{ij}+\Delta K_{ij})\sin(\phi_j + \Delta\phi_j - \phi_i - \Delta\phi_i) = \Omega.$$

Assuming ΔK_{ij} to be infinitesimally small, the change $\Delta\phi_j - \Delta\phi_i$ is described by

$$\begin{aligned}
&\omega_i - \Omega + \sum_j a_{ij}(K_{ij}+\Delta K_{ij}) \times \sin(\phi_j + \Delta\phi_j - \phi_i - \Delta\phi_i) \\
&= \omega_i - \Omega + \sum_j a_{ij}(K_{ij}+\Delta K_{ij})[\sin(\phi_j - \phi_i)\cos(\Delta\phi_j - \Delta\phi_i) \\
&\quad + \cos(\phi_j - \phi_i)\sin(\Delta\phi_j - \Delta\phi_i)] \\
&\approx \omega_i - \Omega + \sum_j a_{ij}(K_{ij}+\Delta K_{ij}) \times [\sin(\phi_j - \phi_i) \\
&\quad + \cos(\phi_j - \phi_i)(\Delta\phi_j - \Delta\phi_i)] \\
&\approx \sum_j a_{ij}\Delta K_{ij}\sin(\phi_j - \phi_i) + a_{ij}K_{ij}\cos(\phi_j - \phi_i) \\
&\quad \times(\Delta\phi_j - \Delta\phi_i) = 0.
\end{aligned}$$

Note that this system of linear equations with variables $\Delta\phi_i$ $(i=1,\ldots,N)$ is degenerate because these variables appear only in the form of $\Delta\phi_j-\Delta\phi_i$. Although, in general, degenerate system of linear equations cannot be solved, this system can be solved as follows. The equation reads

$$M\mathbf{x} = \mathbf{y}, \tag{5}$$

where

$$\mathbf{x} = [\Delta\phi_i],$$

$$\mathbf{y} = \left[\sum_j a_{ij}\Delta K_{ij}\sin(\phi_j - \phi_i)\right],$$

and

$$M = \left(\delta_{ij}\sum_l a_{il}K_{il}\cos(\phi_l - \phi_i) - a_{ij}K_{ij}\cos(\phi_j - \phi_i)\right).$$

Because $M\mathbf{x}=\mathbf{0}$ if $\Delta\phi_1=\Delta\phi_2=\cdots=\Delta\phi_N$, the rank of matrix M is $N-1$. Thus, its eigenvector corresponding to zero ei-

genvalue is $\mathbf{e}=(1,1,\ldots,1)$, and because M is a symmetric matrix, the other eigenvectors are orthogonal to $\mathbf{e}$. Hence, the solution $\mathbf{x}$ exists if $\mathbf{y}$ is orthogonal to $\mathbf{e}$. This condition is satisfied since the coupling matrix is symmetric. Thus, using the specific value decomposition

$$M = U\Sigma U^T,$$

we obtain

$$\mathbf{x} = U\Sigma^+ U^T\mathbf{y},$$

where Σ^+ is the matrix Σ with every nonzero entry replaced by its reciprocal. Therefore, using $K_{ij}=K_{ji}$, we obtain

$$\begin{aligned}\frac{\partial \phi_k}{\partial K_{ij}} = \frac{\partial \phi_k}{\partial K_{ji}} &= \frac{\partial \phi_k}{\partial y_i}\frac{\partial y_i}{\partial K_{ij}} + \frac{\partial \phi_k}{\partial y_j}\frac{\partial y_j}{\partial K_{ji}} \\ &= W_{ki}a_{ij}\sin(\phi_j - \phi_i) + W_{kj}a_{ji}\sin(\phi_i - \phi_j) \\ &= (W_{ki} - W_{kj})a_{ij}\sin(\phi_j - \phi_i),\end{aligned}$$

where W_{kj} is the (k,j) component of the matrix $U\Sigma^+U^T$. Differentiating Q_1 with respect to K_{ij}, we obtain

$$\frac{\partial Q_1}{\partial K_{ij}} = \frac{\partial Q_1}{\partial K_{ji}} = \frac{1}{N^2}\left(-2\sum_k \cos\phi_k \sum_k \sin\phi_k \frac{\partial \phi_k}{\partial K_{ij}} + 2\sum_k \sin\phi_k \sum_k \cos\phi_k \frac{\partial \phi_k}{\partial K_{ij}}\right) = F_{ij}.$$

The optimal direction $\Delta K_{ij}=u_{ij}$ under the constraint Eq. (4) is given by the Lagrange method. Using

$$\sum_{ij}(K_{ij}+u_{ij})^\alpha \approx \sum_{ij} K_{ij}^\alpha + \alpha K_{ij}^{\alpha-1}u_{ij} + \frac{\alpha(\alpha-1)}{2}K_{ij}^{\alpha-2}u_{ij}^2, \tag{6}$$

and assuming $u_{ij} \ll K_{ij}$, we can replace the constraint Eq. (4) with

$$\alpha\sum_{ij} K_{ij}^{\alpha-1}u_{ij} + \frac{\alpha-1}{2}K_{ij}^{\alpha-2}u_{ij}^2 = 0.$$

Differentiation of the function

$$L \approx Q_1 + \mu\alpha\sum_{ij} K_{ij}^{\alpha-1}u_{ij} + \frac{\alpha-1}{2}K_{ij}^{\alpha-2}u_{ij}^2$$

with respect to u_{ij} gives the equation

$$F_{ij} + \mu\alpha[K_{ij}^{\alpha-1} + (\alpha-1)K_{ij}^{\alpha-2}u_{ij}] = 0.$$

Rearranging, we obtain the optimal direction

$$\Delta K_{ij} = u_{ij} = -\frac{1}{\alpha-1}\left(\frac{F_{ij}}{\mu\alpha K_{ij}^{\alpha-2}} + K_{ij}\right).$$

Because the second term does not affect the direction, we can replace it with

$$\Delta K_{ij} = -\frac{F_{ij}}{\mu\alpha(\alpha-1)K_{ij}^{\alpha-2}}$$

and thereby we update K_{ij} with

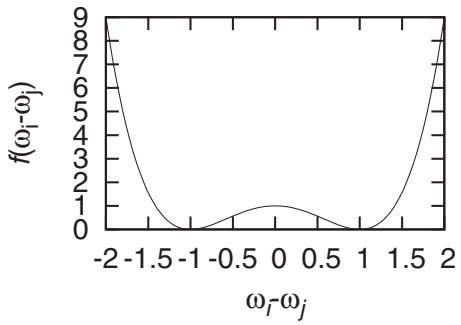

FIG. 1. Penalty function $f(\omega_i-\omega_j)$ for $A=1$ introduces repulsion and attraction among the natural frequencies of the oscillators. This function takes its minima at $\omega_i-\omega_j=\pm 1$.

$$K_{ij} \leftarrow K_{ij} + \epsilon\frac{F_{ij}}{K_{ij}^{\alpha-2}}, \tag{7}$$

and renormalize it with the constraint Eq. (4). Note that, since the approximation in Eq. (6) does not hold for $\alpha=1$, the optimal direction Eq. (7) cannot be used in this case.

B. Optimization with respect to coupling strength and natural frequency

In order to investigate the effect of natural frequencies in the synchronization of phase oscillators, we examine the optimization with respect to not only coupling strength but also the natural frequencies of the oscillators in the network to maximize the optimization function

$$Q_2 = Q_1 - \frac{\lambda}{N^2}\sum_{ij} f(\omega_i - \omega_j), \tag{8}$$

where $f(x)=(x-A)^2(x+A)^2$ and λ is a constant parameter. In the following, we set $A=1$. The first term is the square of the order parameter and the second term is a penalty term, which prevents oscillators from having identical natural frequencies (Fig. 1). We add the second term to the optimization function because maximizing the order parameter without the penalty term while allowing the natural frequencies to vary just makes the oscillators converge to the same natural frequency. The second term introduces repulsion and attraction among the natural frequencies of the oscillators.

Because maximization of the optimization function Eq. (8) can be done by changing K_{ij} and ω_i independently, we can derive the steepest gradient with respect to K_{ij} and ω_i separately. Since the steepest gradient of the optimization function with respect to K_{ij} is given by Eq. (7), it is sufficient for us to derive the steepest gradient with respect to ω_i. Proceeding in the same way as in the derivation of the gradient with respect to K_{ij}, we obtain the differentiation of phase ϕ_j with respect to ω_i,

$$\frac{\partial \phi_j}{\partial \omega_i} = V_{ji},$$

where

$$P\mathbf{z} = \mathbf{w},$$

$$\mathbf{z} = [\Delta\phi_i],$$

$$\mathbf{w} = [\Delta\omega_i],$$

$$P = \left(\delta_{ij}\sum_k a_{ik}K_{ik}\cos(\phi_k - \phi_i) - a_{ij}K_{ij}\cos(\phi_j - \phi_i)\right),$$

$$\mathbf{z} = Y\Xi^+ Y^T\mathbf{w} = V\mathbf{w},$$

and $Y\Xi Y^T$ is a specific value decomposition of P. In a similar way as for M in the previous derivation, P is degenerate and symmetric, and thus $\mathbf{w}$ must be orthogonal to the eigenvector $\mathbf{e}$. We hence set the average of the natural frequencies to 0. Differentiating the optimization function Eq. (8) with respect to ω_i yields the steepest direction,

$$\Delta\omega_i = \frac{\partial}{\partial\omega_i}\left(Q_1 - \frac{\lambda}{N^2}\sum_{jk} f(\omega_j - \omega_k)\right)$$

$$= \frac{1}{N^2}\left(-2\sum_j \cos\phi_j \sum_j \sin\phi_j \frac{\partial\phi_j}{\partial\omega_i} + 2\sum_j \sin\phi_j \sum_j \cos\phi_j \frac{\partial\phi_j}{\partial\omega_i} - 2\lambda\sum_j f'(\omega_j - \omega_i)\right).$$

The natural frequency ω_i is updated by

$$\omega_i \leftarrow \omega_i + \eta\left(\Delta\omega_i - \frac{1}{N}\sum_j \Delta\omega_j\right). \quad (9)$$

The last summation is subtracted from Eq. (9) in order to set the average of the natural frequencies to 0.

III. RESULTS

A. Optimization with respect to coupling strength

Since the present algorithm requires all the oscillators to be phase locked, K_{total} must be large enough at the beginning of the optimization process to allow the oscillators connected by the initial random coupling matrix to be phase locked. To obtain the optimized coupling strength in the network with a small K_{total}, we adopted the following simulation schedule: (i) set K_{total} to a large $K_{\text{total}}^{\text{start}}$ and run the simulation for period T_1 according to Eq. (3) without running the optimization algorithm; (ii) run the simulation and optimization algorithm, decreasing K_{total} from $K_{\text{total}}^{\text{start}}$ to $K_{\text{total}}^{\text{end}}$ linearly for period T_2, that is, $K_{\text{total}} = K_{\text{total}}^{\text{start}} + (t - T_1)(K_{\text{total}}^{\text{end}} - K_{\text{total}}^{\text{start}})/T_2$; and (iii) run the simulation and optimization algorithm without changing K_{total} for period T_3. We updated the coupling strength using Eq. (7) at $t = 10n$, where n is a positive integer, to allow the phase of oscillators to converge to a new equilibrium state in the intervals of updates. In the simulations presented here, the interval of 10 was long enough for the phase of oscillators to converge.

First, we optimized the coupling strength without changing the natural frequency. The all-to-all coupling strengths for the $N = 20$ oscillators were drawn from an uniform distribution and normalized using $K_{\text{total}} = 1$ and $\alpha = 2$. Natural frequency of oscillator i $(i = 1, \ldots, 20)$ was set to $0.05(i - 10.5)$.

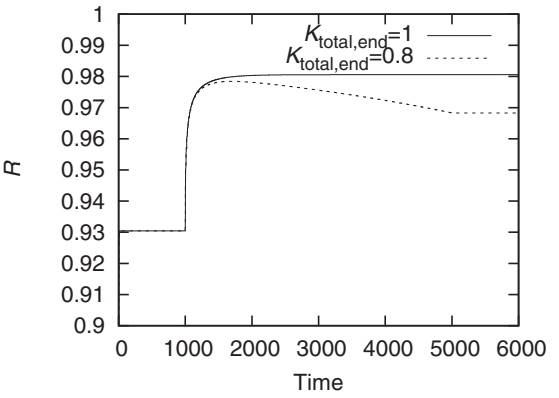

FIG. 2. Order parameter of the oscillators on an all-to-all network improved through optimization. Here the following parameter values were used: $N = 20$, $\alpha = 2$, $\epsilon = 0.1$, $\eta = 0$, $K_{\text{total}}^{\text{start}} = 1$, $T_1 = 1000$, $T_2 = 4000$, and $T_3 = 1000$.

After the phases of oscillators and the order parameter converged in first $T_1 = 1000$, we started to update the coupling strength using Eq. (7) and $\epsilon = 0.1$. We stopped updating the total coupling strength at $t = T_1 + T_2 = 5000$. Figure 2 shows that the order parameter reached 0.98 in the case of $K_{\text{total}}^{\text{end}} = 1$, and 0.97 in the case of $K_{\text{total}}^{\text{end}} = 0.8$ after optimization. After $t = 1500$, the order parameter decreased in the case of $K_{\text{total}}^{\text{end}} = 0.8$ since K_{total} started to decrease at $t = 1000$.

Figure 3 shows the final state of the network for $K_{\text{total}}^{\text{end}} = 1$. The coupling strength of a link became large only when the difference of natural frequencies of the oscillators connected by this link was large, and thus the oscillators with natural frequencies far from the average gained strong connections. This is a natural result due to the following reasons. Assigning a large weight to the coupling between two oscillators with close natural frequencies results in little increase in the order parameter, whereas assigning a large weight to the link between oscillators with very different natural frequencies improves the order parameter more effectively. In other words, the cost-efficient way is to concentrate the coupling between two oscillators whose natural frequencies are very different from the average in opposite directions. We

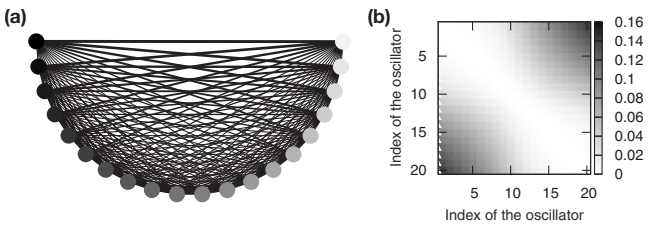

FIG. 3. Final coupling strength of the network with $K_{\text{total}}^{\text{end}} = 1$ in Fig. 2. (a) The oscillators are indicated by circles and their natural frequencies are indicated by gray levels. Black and white correspond to lowest and highest natural frequencies, respectively. Oscillators with high and low natural frequencies have strong connections indicated by thick lines. (b) Large coupling strength is found only on links connecting two oscillators with large deviation of the natural frequency from the mean. The coupling strength between oscillators with close natural frequencies is weak (diagonal white belt).

TABLE I. Natural frequencies of the optimized two-oscillator system.

	Large λ	Small λ
$\lvert\omega_1-\omega_2\rvert$	$\approx A$	≈ 0
	Large K_{total}	Small K_{total}
$\lvert\omega_1-\omega_2\rvert$	$\approx A$	≈ 0

found that this result held for systems with the distribution of natural frequencies other than a uniform distribution, such as a Gaussian or a Lorentzian.

When we started the optimization process from different initial coupling matrices, the resultant coupling converged to almost the same matrices. The present optimization algorithm hence is expected to be able to reach the global maximum.

B. Optimization with respect to coupling strength and natural frequency

Next, we examined the outcome of optimizing the function Eq. (8) by changing both coupling strength K_{ij} and natural frequency ω_i. We updated the coupling strength and natural frequency using Eqs. (7) and (9) at $t=10n$ ($T_1<t$), where n is a positive integer. To understand the essential factors affecting the resultant network structure, let us examine how parameters λ and K_{total} change the natural frequencies of oscillators in the optimized network of two oscillators before presenting the simulation result. If λ is large and thereby the first term of Eq. (8) can be ignored, the optimization function Eq. (8) is maximized by setting the natural frequencies of the oscillators to $-A/2$ and $A/2$, because the penalty function $f(x)$ of the natural frequency has minima at $x=\pm A$. In contrast, if λ is small and we can ignore the second term, the natural frequencies of all oscillators tend to converge to the same value in order to facilitate synchronization. Large K_{total} allows the system of two oscillators with greatly differing natural frequencies to attain $R^2\approx 1$, and thus the optimization function Eq. (8) can be approximated by

$$Q_2 \approx 1 - \frac{\lambda}{N^2}\sum_{ij} f(\omega_i - \omega_j). \tag{10}$$

Under this condition, maximizing Eq. (10) sets the natural frequencies of the oscillators to $-A/2$ and $A/2$. On the other hand, if K_{total} is small, the natural frequencies of oscillators converge to a single value in order to improve the first term of Eq. (8) because otherwise a small K_{total} may not allow the oscillators to be phase locked. Thus, a large K_{total} and a large λ make the oscillators take two natural frequencies, and a small K_{total} and a small λ facilitate the convergence of natural frequencies to one single value (Table I).

Next, let us examine whether or not the qualitative results described above are applicable to systems with more than two oscillators. Figure 4(a) shows the phase diagram for the optimized network of 50 oscillators coupled in an all-to-all manner. In this diagram, the total coupling strength K_{total} at the end of the simulation $K_{\text{total}}^{\text{end}}$ ranges from 1 to 5 and λ

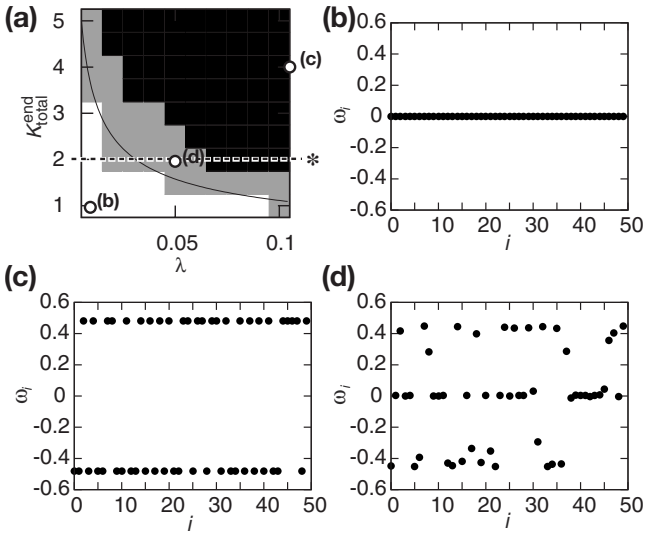

FIG. 4. Optimization of the oscillators for an all-to-all network with respect to coupling strength and natural frequency. (a) Phase diagram of the optimized network. Simulation results are classified into the (almost) symmetric two-group state (dark gray), the one-group state (white), and the other states (light gray), which include the asymmetric two-group state and the multigroup state. The black line shows the theoretical border of one- and two-group states. More detailed simulation results for $K_{\text{total}}^{\text{end}}=2$ (dashed line) are shown in Fig. 5. (b)–(d) Examples of the natural frequencies of oscillators after optimization. We present the one-group state (λ $=0.01$ and $K_{\text{total}}=1$) in (b), the two-group state (λ$=0.1$ and K_{total} $=4$) in (c), and a state that is classified in neither group (λ$=0.05$ and $K_{\text{total}}=2$) in (d). Here the following parameter values were used: $N=50$, $\alpha=2$, $\epsilon=10$, $\eta=5$, $A=1$, $K_{\text{total}}^{\text{start}}=20$, $T_1=100$, $T_2=1900$, and $T_3=8000$.

ranges from 0.01 to 0.1. The resultant networks are classified into three categories, one-group state, two-group state, and miscellaneous. The natural frequencies of the oscillators in the one-group state [Fig. 4(b)] converged to the same value, and in the two-group state [Fig. 4(c)] the natural frequencies of the oscillators converged to values close to $-A/2$ or $A/2$. In the two-group state, couplings linking two oscillators in the same group converged to zero, and couplings linking two oscillators from different groups converged to the same value (not shown). Note that λ in the region where two-group states were observed is larger than that in the one-group region, and K_{total} in the region where two-group states were observed is larger than that in the one-group region, as in the two-oscillator networks considered above. In addition, there were many networks which were classified as neither one-group nor two-group states [Fig. 4(d)].

In contrast to the optimization with respect to only K_{ij}, the optimization with respect to both K_{ij} and ω_i did not necessarily converge to unique K_{ij}s and ω_is. In the two-group state, whether the natural frequency of oscillator i converged to $A/2$ or $-A/2$ depended on the initial connections and natural frequencies.

Whether the two-group state is more favorable than the one-group state can be discriminated by analytical calculation. We derive the optimization function of Eq. (8) in two-group and one-group states and compare them to estimate

which is more favorable. To obtain the optimization function of a two-group state in which two groups have natural frequencies ω and $-\omega$, and phases ϕ and $-\phi$, we can derive the equations

$$2mK^{\alpha} = K_{\text{total}}^{\alpha},$$

$$\omega + nK \sin(-2\phi) = 0,$$

where we assume a total of m connections have the same coupling strength K, the oscillators have n connections each to the oscillators in the other group, and the two groups have the same number of oscillators, $N/2$. In the case of all-to-all coupling and two-dimensional (2D) lattice coupling, these parameters take the values $n=N/2$ and $m=Nn/2=N^2/4$, and $n=4$ and $m=2N$, respectively. If the maximum of the optimization function of the two-group state,

$$\begin{aligned} Q_2^{\text{two}}(\phi) &= R^2 - \frac{\lambda}{N^2}\sum_{ij} f(\omega_i - \omega_j) \\ &= \frac{1}{N^2}\left[\left(\sum_i \cos\phi_i\right)^2 + \left(\sum_i \sin\phi_i\right)^2\right] \\ &\quad - \frac{\lambda}{N^2}\sum_{ij} f(\omega_i - \omega_j) = \frac{1}{N^2}(N^2\cos^2\phi) \\ &\quad - \frac{\lambda}{N^2}N\left(\frac{N}{2}f(2\omega) + \frac{N}{2}f(0)\right) \\ &= \cos^2\phi - \frac{\lambda}{2}(f(2\omega) + f(0)) \\ &= \cos^2\phi - \frac{\lambda}{2}\left\{f\left[2n\left(\frac{K_{\text{total}}^{\alpha}}{2m}\right)^{1/\alpha}\sin 2\phi\right]\right. \\ &\quad \left. + f(0)\right\}, \end{aligned}$$

is larger than that of the one-group state, $Q_2^{\text{one}}=1-\lambda f(0)$, the two-group state becomes stable. Because $Q_2^{\text{two}}(\phi)$ is an even function and $Q_2^{\text{two}}(0)=Q_2^{\text{one}}$, the sign of the second derivative of $Q_2^{\text{two}}(\phi)$ at $\phi=0$ determines the stability of the two-group state. Specifically, if $d^2Q_2^{\text{two}}/d\phi^2|_{\phi=0}>0$, the two-group state is more favorable than the one-group state, and if $d^2Q_2^{\text{two}}/d\phi^2|_{\phi=0}<0$, two-group state is less favorable. Because $d^2Q_2^{\text{two}}/d\phi^2=-2+32\lambda A^2n^2(\frac{K_{\text{total}}^{\alpha}}{2m})^{2/\alpha}$ at $\phi=0$, this is the border of the two- and one-group states. When the oscillators are coupled in an all-to-all manner, in the two-group state, an oscillator in a group has $n=N/2$ connections to the oscillators in the other group, and the connection strength to the oscillators in the same group becomes 0. Thus, the total number of connections is $m=N^2/4$, and the border of the one- and two-group states is given by $8\lambda K_{\text{total}}^2=1$ for $\alpha=2$ and $A=1$ [solid line in Fig. 4(a)]. This theoretical border is consistent with the simulation results. Large λ and K_{total} favor the two-group state and small λ and K_{total} favor the one-group state, as discussed above.

Next, we examined what takes place at the border of the one- and two-group states in the network with $K_{\text{total}}^{\text{end}}=2$ [dashed line with asterisk on the side in Fig. 4(a)]. We found

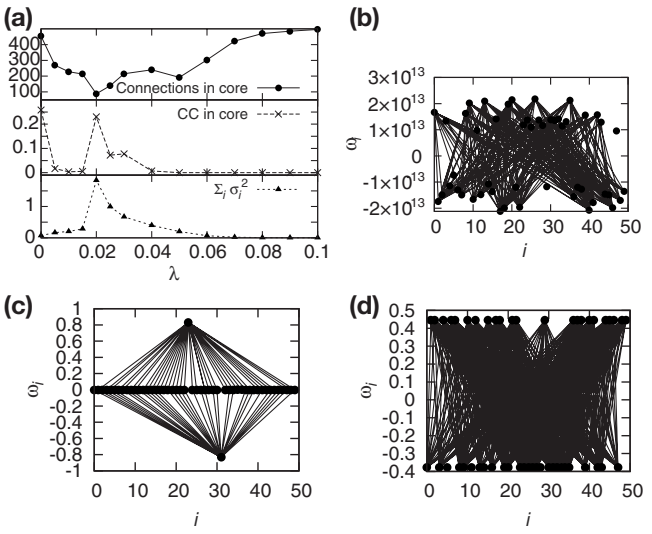

FIG. 5. Number of connections in 0.8-core, clustering coefficient (CC), and strength S_i of the nodes exhibiting critical behavior at $\lambda \approx 0.02$ in a network with all-to-all connection optimized with $K_{\text{total}}^{\text{end}}=2$ (a). The optimized network structures with $\lambda=0.01$, 0.02, and 0.1 are shown in (b), (c), and (d), respectively. Here the same parameter values as in Fig. 4 were used.

that most of coupling strength is gained by a relatively small number of connections in networks optimized with $\lambda=0.02$. To quantify this observation, we define the p-core $\mathcal{C}_p$ of a weighted network as the smallest set of strongest connections which satisfies

$$\sum_{(i,j)\in\mathcal{C}_p, i<j} 2K_{ij}^{\alpha} \geqslant pK_{\text{total}}^{\alpha},$$

where α is set to 2. In Fig. 5(a), the natural frequencies of oscillators are indicated by the y coordinate of the dots, and connections in the 0.8-core are indicated by lines, which are fewer in the networks optimized with $\lambda=0.02$ than in those with $\lambda=0.01$ and $\lambda=0.1$. Optimizing $M=20$ networks with all-to-all connectivity starting from random connection strengths and natural frequencies, we found that the number of connections in the 0.8-core was a minimum at $\lambda=0.02$ [Fig. 5(a)]. The middle panel of Fig. 5(a) shows that the clustering coefficient of the 0.8-core peaks at this point, and starts to decrease until $\lambda=0.04$ where it vanishes. The clustering coefficient in the core vanishes at large λ because the network takes the two-group state, and in this state connections among the oscillators in the same group are weakened [Fig. 5(d)]. The network optimized with $\lambda=0.01$ [Fig. 5(b)] also exhibits a small clustering coefficient because strong connections are formed only between the oscillators whose natural frequencies are of opposite signs, although the natural frequencies of all oscillators are close to zero and thereby this network is classified into the one-group state. In contrast, the clustering coefficient of the network optimized with $\lambda=0.02$ can be larger. With this parameter, in some networks the natural frequencies of oscillators i and j converge to finite values ω_i and ω_j ($\omega_i<0<\omega_j$), and the natural frequencies of other oscillators vanish [Fig. 5(c)]. In this case, the connection between oscillators i and j is strengthened, and

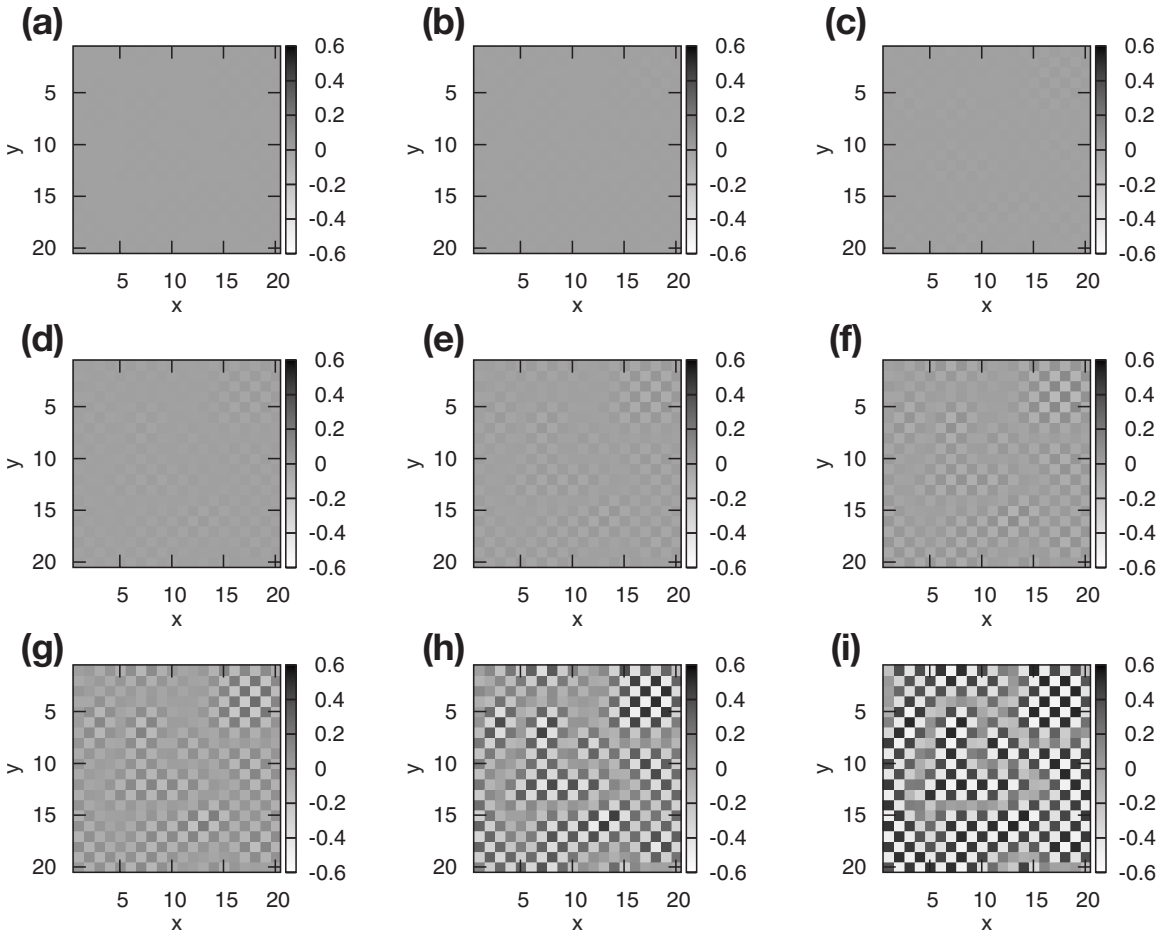

FIG. 6. Natural frequencies of the oscillators on a lattice structure. Here the following parameter values were used: $N=400$, $\alpha=2$, $\epsilon=1$, $\eta=4$, $K_{\text{total}}^{\text{start}}=2000$, $K_{\text{total}}^{\text{end}}=32$, $T_1=100$, $T_2=400$, and $T_3=99\,500$. Penalty parameter λ was set to (a) 0.001, (b) 0.002, (c) 0.003, (d) 0.004, (e) 0.005, (f) 0.006, (g) 0.007, (h) 0.01, and (i) 0.02. Theoretical border of the one-group and two-group states is $\lambda=0.0061$. All the systems presented in this figure started from the same initial condition.

oscillators k with natural frequencies close to zero are connected by strong links to both oscillators i and j. This structure contains a large number of triangles composed of the three oscillators i, j, k. This means that the clustering coefficient grows larger in this network structure. This abrupt change in the clustering coefficient at $\lambda=0.02$ suggests that a phase transition occurs at $\lambda\approx0.02$. We now examine the change of the network structure further, and define $K_{ij}^{(m)}$ as the optimized connection strength between nodes i and j in the network starting from the mth initial condition and $S_i^{(m)}$ as the strength of node i, in the mth network as

$$S_i^{(m)}=\sum_j (K_{ij}^{(m)})^{\alpha}.$$

Measuring the variance of the strength of node i,

$$\sigma_i^2=\frac{1}{M}\sum_m (S_i^{(m)})^2-\left(\frac{1}{M}\sum_m S_i^{(m)}\right)^2,$$

where the summation is taken over M initial conditions, we found that the summation of the variance $\Sigma_i\sigma_i^2$ has a peak at $\lambda\approx0.02$ [Fig. 5(a)]. The peaks in the variance and clustering coefficient, and the drop in the number of connections in the core, indicate a phase transition from a one-group to a two-group state in the optimized network structure.

In the previous paragraphs, we described the results for an all-to-all network. Next, we examined whether or not we can generalize this relationship between the parameter λ and the group formation of natural frequencies to other network structures. We take as an example a 2D lattice of 20×20 oscillators, each of which is connected to oscillators on the top, bottom, left, and right. We use periodic boundary conditions under which the topmost oscillators are connected to the bottommost oscillators and the leftmost and rightmost oscillators are also connected. Figure 6 shows the natural frequencies of the oscillators in this system at the end of the optimization process. In this simulation, K_{total} was fixed to 32 and λ ranged from 0.001 to 0.02. The natural frequencies converged to zero for small λ, and they showed frustrated checker patterns, which correspond to a two-group state, for large λ. Thus, as in an all-to-all network, the network takes the two-group state for large λ whereas a small λ favors the one-group state. The transition from the one-to two-group state takes place around the parameter $\lambda=0.0061$ predicted by the above analysis using $n=4$ and $m=2N$. Hence, the relationship between the parameter λ and the group forma-

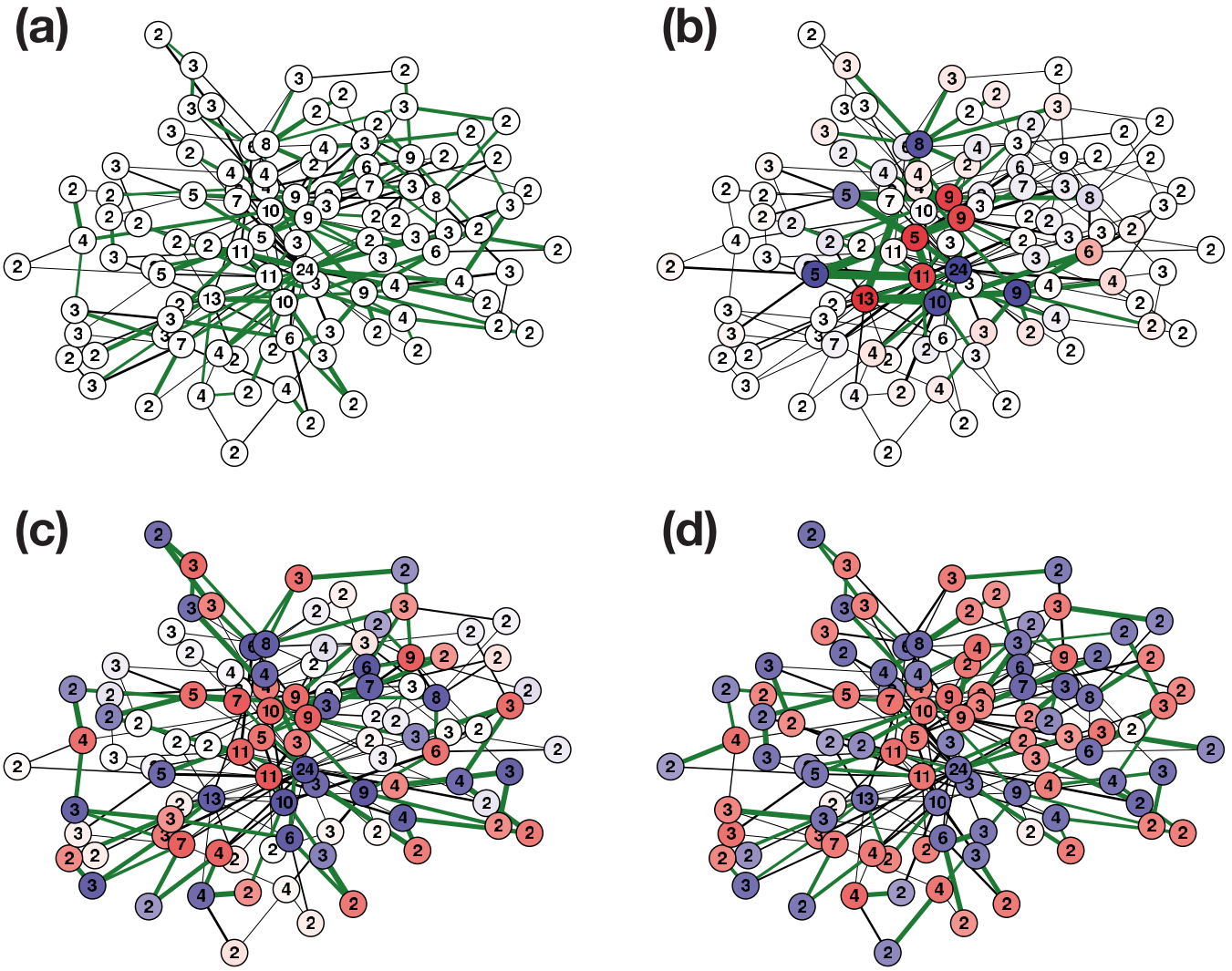

FIG. 7. (Color online) Optimized connections and natural frequencies of the oscillators on a Barabási-Albert network. The oscillators are indicated by circles in which their degree numbers are shown. Their natural frequencies are indicated by colors. Positive, negative, and zero natural frequencies are indicated by red, blue, and white respectively. Connections in 0.8-core (see definition in the main text) are indicated by green lines. Here the following parameter values were used: $N=100$, $\alpha=2$, $\epsilon=10$, $\eta=5$. $K_{\mathrm{total}}^{\mathrm{start}}=1000$, and $K_{\mathrm{total}}^{\mathrm{end}}=10$. Penalty parameter λ was set to (a) 0.001, (b) 0.01, (c) 0.1, and (d) 0.1.

tion of natural frequencies holds for the 2D lattice.

Finally, we examined the structure emerging through the optimization of synchronization on a scale-free network. We optimized the synchronizability of a Barabási-Albert network with 100 nodes (Fig. 7). In this simulation, we adopted the following simulation schedule: (i) set K_{total} to $K_{\mathrm{total}}^{\mathrm{start}}=1000$ and run the simulation for period $T_1=100$ according to Eq. (3) without running the optimization algorithm; (ii) run the simulation and optimization algorithm, decreasing K_{total} to $K_{\mathrm{total}}^{\mathrm{middle}}=100$ linearly for period $T_2=100$; (iii) run the simulation and optimization algorithm, decreasing K_{total} to $K_{\mathrm{total}}^{\mathrm{end}}=10$ linearly for period $T_2'=1900$; and (iv) run the simulation and optimization algorithm without changing K_{total} for period $T_3=98\,000$. We found that all natural frequencies converged to zero if $\lambda=0.001$, and that almost all natural frequencies converged to around $\pm A/2$ if $\lambda=1$, similarly to the behavior observed in networks with all-to-all coupling and lattice structures. However, the networks optimized using $\lambda=0.01$ and $\lambda=0.1$ cannot be classified into the one-group state or the two-group state. In these networks, the natural frequencies of oscillators with large degree numbers tended to converge to a value far removed from the mean, whereas those of oscillators with small degree numbers vanished (Fig. 8). This is not the case with the one-group and two-group networks resulting from the optimization with $\lambda=0.001$ and $\lambda=1$, which exhibited a rather uniform degree-natural frequency relationship. In addition, we found that a relatively small number of connections gained most of the coupling strength in the networks optimized with $\lambda=0.01$ [Fig. 7(b)] and 0.1 [Fig. 7(c)]. In Fig. 7, connections in the 0.8-core, indicated by green lines, are fewer in the networks optimized with $\lambda=0.01$ [Fig. 7(b)] than in those with $\lambda=0.001$ [Fig. 7(a)] and 1 [Fig. 7(d)]. Optimizing $M=20$ networks with the same topological structure starting from random connection strengths and natural frequencies, we found that the number of connections in the 0.8-core was minimal at $\lambda\approx 0.008$ (Fig.

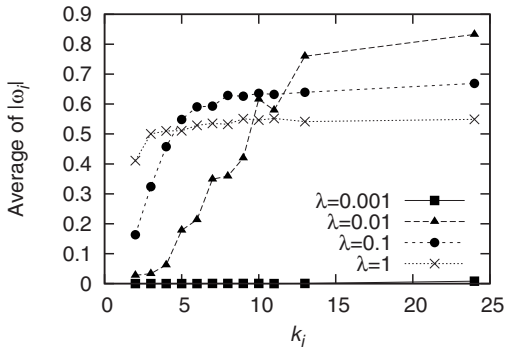

FIG. 8. Average of $|\omega_i|$ as a function of k_i tends to be monotonically increasing. In this simulation, the same parameter values, network topology, and optimization schedule as in Fig. 7 were used.

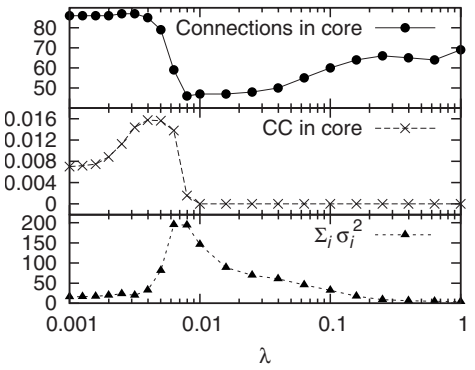

FIG. 9. Number of connections in 0.8-core, clustering coefficient (CC), and strength S_i of the nodes exhibiting a critical behavior at $\lambda \approx 0.008$ in a scale-free network. Clustering coefficient of the whole network is 0.049. In this simulation, the same parameter values, network topology, and optimization schedule as shown in Fig. 7 were used.

9, top). The middle panel of Fig. 9 shows a steep decrease in, and subsequent vanishing around $\lambda=0.01$, of the clustering coefficient of the 0.8-core. This is in sharp contrast to the case with an all-to-all network, because in an all-to-all network a peak of the clustering coefficient was observed at the value of λ where the number of connections in the core is minimal. However, in the same way as in the all-to-all network, this suggests that an abrupt structural change occurs at $\lambda \approx 0.008$. The summation of the variance $\Sigma_i \sigma_i^2$ has a peak at $\lambda \approx 0.008$ (Fig. 9, bottom). We confirmed that this peak coincided with the sharp declines of the number of connections in the core and the clustering coefficient in the networks with larger and smaller number of nodes. These peaks and declines suggest that there takes place a phase transition of the network structure obtained through the optimization of synchronization on a scale-free network.

IV. DISCUSSION

The optimization of the degree of synchronization of oscillators on a network with a given structure was discussed in this paper. One of the advantages of our approach over previous ones is that the present algorithm allows us to understand how the weights should be distributed in the network in order to maximize synchronization. In our study, the relationship between connection strength and natural frequency in networks favorable for synchronization was revealed by our optimization algorithm. More specifically, strongly connecting oscillators with largely differing natural frequencies optimizes the synchronization. This property, which would be useful in application for real-world systems, has not been paid much attention in the previous works considering large random scale-free and Erdös-Renyi networks.

In addition, we observed the transition of the optimal network structure between the one- and two-group states. This transition was observed in networks with all-to-all, lattice, and scale-free network topologies. We confirmed that in both all-to-all and scale-free networks, the number of connections in the core decreased at the border of these two states and the variability of the optimized network structure has a peak at this border. In contrast, at this border, the clustering coefficient has a peak in the all-to-all network, whereas it showed a sharp drop in the scale-free network. This difference needs further investigation.

Our algorithm has some limitations. First, our optimization algorithm is not applicable to systems with $\alpha=1$. This is because the approximation Eq. (6) cannot be used in this case. For the system with $\alpha>1$, we optimized the coupling strength of the network using Eq. (7) and found that the order parameter was maximized when links between two oscillators with greatly different natural frequencies had strong connections, as we saw in the system with $\alpha=2$ (data not shown).

Second, our algorithm assumes all oscillators in the system are phase locked. Thus, optimization through this algorithm does not necessarily generate the network structure in which oscillators with random phases rapidly converge to a phase-locked state. Further work is required to characterize the network structure which facilitates fast synchronization.

Third, in the optimization with respect to natural frequency, we used the optimization function Eq. (8). Since the generated patterns depend not only on the parameters λ and K_{total} as we saw in the previous section, but also on the penalty function f, further work will be required to characterize the synchronization of the oscillators on the weighted network in a more general situation.

In this paper, we derived an optimization algorithm for the oscillators with the coupling function $\sin(\phi_j-\phi_i)$ because it is the simplest and most intensively studied coupling function for oscillator systems, and not because the optimization functions for the other coupling functions cannot be derived. Optimization algorithms for systems with more complex coupling functions can be derived. These algorithms will answer the question of how to assign strong connections in individual physical, chemical, and biological systems with a given structure and coupling function. In addition, our algorithm will be useful not only in constructing highly synchronized networks, but also in examining to what extent the connection strength of a given network is optimized for synchronization.

[1] Y. Kuramoto, *Chemical Oscillations, Waves, and Turbulence* (Springer-Verlag, Berlin, 1984).
[2] H. Daido, Prog. Theor. Phys. **88**, 1213 (1992).
[3] J. A. Acebrón, L. L. Bonilla, C. J. P. Vicente, F. Ritort, and R. Spigler, Rev. Mod. Phys. **77**, 137 (2005).
[4] Y. Moreno and A. F. Pacheco, Europhys. Lett. **68**, 603 (2004).
[5] Y. Moreno Vega, M. Vázquez-Prada, and A. F. Pacheco, Physica A **343**, 279 (2004).
[6] T. Ichinomiya, Phys. Rev. E **70**, 026116 (2004).
[7] D.-S. Lee, Phys. Rev. E **72**, 026208 (2005).
[8] J. G. Restrepo, E. Ott, and B. R. Hunt, Phys. Rev. E **71**, 036151 (2005).
[9] J. Gomez-Gardenes, Y. Moreno, and A. Arenas, Phys. Rev. Lett. **98**, 034101 (2007).
[10] M. E. J. Newman, Phys. Rev. E **64**, 016131 (2001).
[11] A. Barrat, M. Barthélemy, R. Pastor-Satorras, and A. Vespignani, Proc. Natl. Acad. Sci. U.S.A. **101**, 3747 (2004).
[12] R. Ferrer i Cancho and R. V. Solé, Santa Fe Institute Technical Report No. 01-03-016, 2001 (unpublished), http://ideas.repec.org/p/wop/safiwp/01-03-016.html
[13] M. Chavez, D.-U. Hwang, A. Amann, H. G. E. Hentschel, and S. Boccaletti, Phys. Rev. Lett. **94**, 218701 (2005).
[14] F. Sorrentino, M. di Bernardoa, G. Huerta Cuéllar, and S. Boccaletti, Physica D **224**, 123 (2006).